

A lightweight feedback-controlled microdrive for chronic neural recordings

A Jovalekic^{*1}, S Cavé-Lopez^{*1}, A Canopoli¹, J M Ondracek², A Nager¹, A L Vyssotski¹ and R H R Hahnloser^{1,3}

¹Institute of Neuroinformatics, University of Zurich and ETH Zurich, 8057 Zurich, Switzerland and Neuroscience Center Zurich (ZNZ), 8057 Zurich, Switzerland.

²Max Planck Institute for Brain Research, Max von Laue Str. 4, 60438 Frankfurt am Main, Germany.

^{*}Joint first authorship

E-mail: rich@ini.ethz.ch

Abstract. Objective: Chronic neural recordings have provided many insights into the relationship between neural activity and behavior. We set out to develop a miniaturized motorized microdrive that allows precise electrode positioning despite possibly unreliable motors.

Approach: We designed a feedback-based motor control mechanism. It contains an integrated position readout from an array of magnets and a Hall sensor.

Main results: Our extremely lightweight (<1 g) motorized microdrive allows remote positioning of both metal electrodes and glass pipettes along one motorized axis. Target locations can be defined with a range of 6 mm and they can be reached within 1 μ m precision. The incorporated headstage electronics are capable of both extracellular and intracellular recordings. We included a simple mechanism for repositioning electrodes in three dimensions and for replacing them in midst operation. We present neural data from different premotor areas of adult and juvenile zebra finches.

Significance: Our findings show that feedback-based microdrive control requires little extra size and weight, suggesting that feedback-based control can be incorporated into more complex multi-electrode designs.

³ rich@ini.ethz.ch

1. Introduction

Insights from electrophysiological studies have provided milestones in our understanding of brain functions. Classically, methods can be divided into extracellular or intracellular recording techniques. Extracellular recordings are widely used in awake and freely moving animals, as this approach allows studying neural activity on a single-neuron level with stability for several hours and in some cases up to several days or even weeks (McCasland 1987, O'Keefe and Dostrovsky 1971, Fee and Leonardo 2001, Lever *et al* 2002). Extracellular recordings have allowed researchers to link action potential activity with behavior, such as the discovery of hippocampal place cells (O'Keefe and Dostrovsky 1971) and entorhinal grid cells (Hafting *et al* 2005) in rodents, or the precise and sparse firing patterns of premotor neurons in singing birds (Prather *et al* 2008, Dave *et al* 1998, Hahnloser *et al* 2002, Kozhevnikov and Fee 2007).

Intracellular recordings provide a tool to investigate subthreshold mechanisms such as subthreshold potentials and synaptic integration (Schneider *et al* 2014), but they can also be used for single-unit stimulation in search of motor correlates (Brecht *et al* 2004). Intracellular recordings in freely behaving animals were pioneered only recently: Lee *et al* (2006) were able to obtain whole-cell recordings in non-head-fixed, freely moving rats. Long *et al* (2010) have improved the intracellular approach and significantly reduced the weight of the recording device from 20 g down to 1.6 g. These latter authors were able to use sharp pipettes mounted on their lightweight device to record intracellularly in freely moving and singing zebra finches.

In freely behaving animals, electrodes are either chronically implanted at a fixed position (McCasland & Konishi 1981; Tolia *et al.* 2007; Yin *et al.* 2014; Foster *et al.* 2014) or are attached to small micromanipulators (microdrives) that allow electrode displacement in the brain. Microdrives have been developed in many different forms and have been widely used to record neurons in small vertebrates such as rodents and songbirds. Typically, microdrives are designed in such a way to be as light and small as possible in order not to interfere with normal behavior.

Microdrives can roughly be divided into those that are manually adjustable (Ainsworth and O'Keefe 1977, Deadwyler *et al* 1979, Venkatachalam *et al* 1999) and those that are motorized (Yamamoto and Wilson 2008, Yang *et al* 2011, Fee and Leonardo 2001). Manually adjustable microdrives have the benefit that they can easily be manufactured and are typically more lightweight than their motorized counterparts. In fact, manual microdrives are the state of the art tools in chronic preparations with rodents. There, multiple microwires (e.g. multiple tetrodes) are inserted into the brain and advanced daily in small steps of usually 50-100 μm . Depending on the design, all recording electrodes are advanced together or are moved independently (Battaglia *et al* 2009). Recently, non-motorized microdrives have been combined with microelectrode arrays to unidirectionally adjust electrode positions in the brain (Márton *et al.* 2016). In brain areas with dense neuron populations, low-impedance microwire electrodes do not unambiguously reveal single-neuron activity, which is why often higher impedance electrodes are preferred.

Non-motorized drives exhibit a number of limitations especially in songbirds as handling and restraining of birds can suppress singing behavior significantly (Fee and Leonardo 2001). Additionally, restraining and handling birds can lead to loss of single-cell activity. To circumvent these limitations, various types

of motorized microdrives have been developed that allow displacing of electrodes without disrupting the animal behavior. Limitations of many designs are that electrode position cannot be read out, which in combination with unreliable miniature motors prevents precise positioning of electrodes. Due to lack of feedback, estimated recording locations are prone to error accumulation. In multi-serial recordings with intermittent electrode movement it is not possible to reconstruct the position of each recorded cell, which is one major drawback of no-feedback ("open-loop") motor controllers. To circumvent these drawbacks we present a new microdrive design with a closed-loop electrode positioning mechanism. Another useful property of some microdrives is the possibility in chronic experiments of exchanging or repositioning the electrode (Márton et al. 2016). The microdrive we designed allows replacement and repositioning of either metal electrodes for extracellular recordings or glass pipettes for juxta or intracellular recordings.

Here we present a new technical approach for performing extracellular or intracellular recordings using the same motorized microdrive weighing less than 1 g. The device offers the following benefits: First, it allows recording neural data with either metal electrodes or glass pipettes. Second, it uses a precise position readout therefore implementing a closed-loop remote electrode positioning mechanism (along the dorsoventral axis), thus allowing precise advancement of microelectrodes into the brain. Third, it permits replacement and repositioning of electrodes during the experiment in the mediolateral and anteroposterior axes, increasing the yield of recordings. We present pilot extracellular recordings in adult and juvenile birds in the premotor area RA (robust nucleus of the arcopallium) and in HVC (proper name), as well as intracellular recordings in field L. Last but not least, adaptations of the design allow the device to be used as a low-cost micromanipulator.

2. Methods

2.1. Microdrive components

Rendered images and photographs of an assembled microdrive are shown in figure 1. The functional microdrive consists of four basic parts: 1) a mechanical scaffold (consisting of top and bottom mounts connected by berylco tubes), 2) a shuttle unit with a piezo-motor (SQL-RV-1.8, New Scale Technologies Inc., <http://www.newscaletech.com/>), 3) a custom-made flexboard circuit board for intracellular and extracellular recordings with an integrated position sensor and motor controller for closed-loop motor control, and 4) a carrier (probe holder).

The weight of an assembled and functional microdrive including a motor, a flexboard, and a glass pipette is only 0.98 g, which is lighter than previously published designs with similar features (Lee *et al* 2006, Lee *et al* 2009, Fee and Leonardo 2001, Yang *et al* 2011). The weights of individual parts are reported in table 1. The size of the drive is 11.1 x 10.9 x 3.5mm. All milled parts were designed with a 3D CAD software (Solidworks, Solidworks) and manufactured in university workshops. Apart from the microdrive holder that was made of brass and the berylco tubes and berylco springs, all parts were made of Torlon® polyamide-imide (Torlon 4203, Solvay, <http://www.solvayplastics.com>). Torlon was chosen because of its exceptional long-term strength and stiffness up to 275°C. Machine drawings of the individually manufactured components are shown in Appendix A of the supplementary data.

The four basic parts of the microdrive are introduced in the following sections. A detailed description of how to assemble the microdrive and a list of components and machine drawings of the single components can be found in Appendix A and B of the supplementary data.

Table 1. Microdrive component weights.

Weight	Components
0.76 g	Assembled Microdrive
0.09 g	Flexboard circuit with motor controller, position sensor and amplification cascade for extracellular and intracellular recordings
0.21 g	Piezo motor SQL-RV-1.8 with customised connective flexboard
0.98 g	Total weight

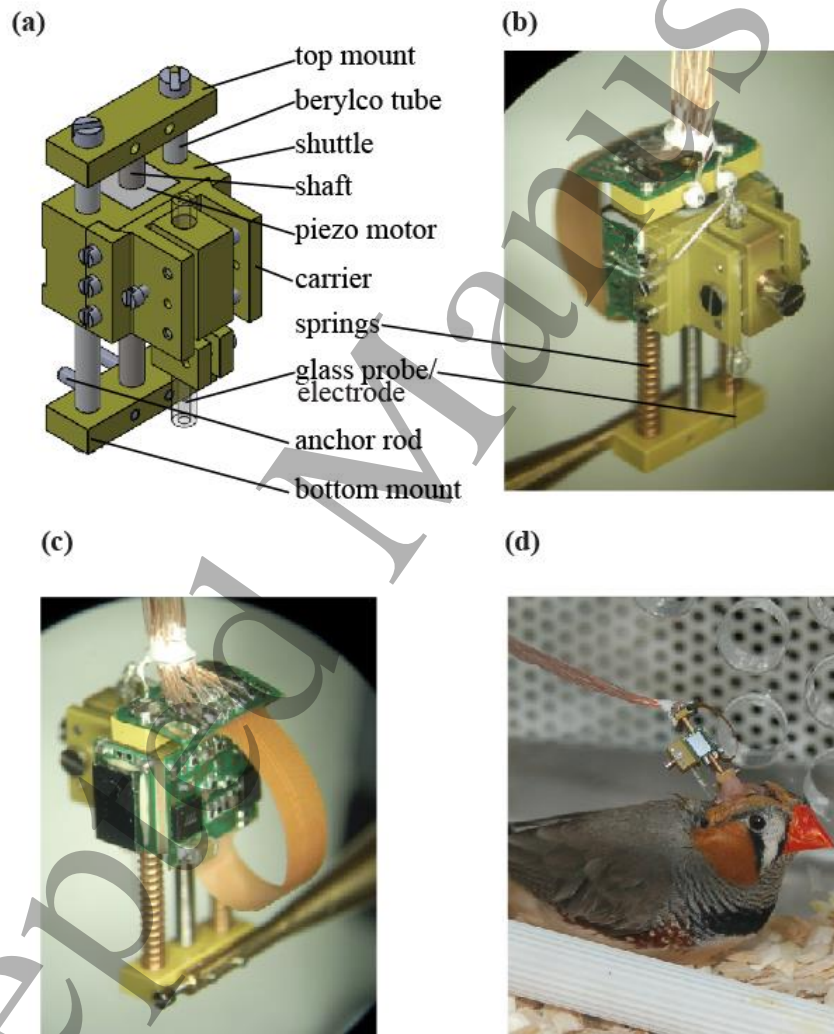


Figure 1. Rendered images and photographs of the microdrive. (a) Rendered 3D view of mechanical parts. (b) Photograph of assembled microdrive (front view) with attached flexboard (green) and inserted electrode. (c) Photograph of assembled microdrive (back view) with attached flexboard. (d) Photograph of the microdrive implanted on a bird's head.

2.1.1. The mechanical scaffold (see figure 2a)

The mechanical scaffold guides the movement of the shuttle and allows head-fixing the animal. It is assembled by connecting two berylco tubes (length 13.8 mm, outer diameter 0.99 mm, NGK BERYLCO, <http://www.ngkbf.com>) with precision screws (M06C, Bergeon, <http://www.bergeon.ch>) to a top and a bottom mount made of Torlon®. Berylco high-precision tubes were chosen because the material combines three desirable properties: 1) it is non-magnetic, 2) it has an excellent corrosion resistance, and 3) it has a high electrical conductivity. For example, the latter property was exploited to route reference and ground signals directly to the flexboard. We inserted 9 micromagnets (Samarium-Cobalt magnets, 1 mm length, 0.0032 g weight per magnet, high Curie temperature, AIC magnets Ltd., <http://www.aicengineering.com>) into one of the berylco tubes, which were later used to read out the shuttle position (see section 3: headstage circuit). Because the piezo motor operates optimally with an axial force between 5 g and 20 g, we used springs to create an appropriate load. Springs were made of berylco roundwire (spring inner diameter: 1.15 mm, resilience 0.143 N, La manufacture, <http://www.lamanufacture.ch/>). To allow head-fixing animals at the bottom or top of the microdrive without a stereotax, two rods were attached either to the top or bottom mounts.

2.1.2. Shuttle with piezo motor (see figure 2b)

A commercial piezo motor (SQL-RV-1.8, New Scale Technologies Inc., <http://www.newscaletech.com/>) with a resonant frequency of 172 kHz was used to move a shuttle up and down the microdrive scaffold. The motor's operation is based on a threaded screw (shaft) and a mating nut, in which ultrasonic vibrations cause the screw to turn. The small dimensions of 2.8 x 2.8 x 6 mm and the weight of only 0.16 g make the motor very suitable for our application. The standard shaft is 12 mm long and offers a 6 mm travel range which is appropriate to reach many recording sites in a small animal's brain (for deeper brain regions it is possible to use longer shafts offering larger travel ranges). Attached to the motorized shuttle is a carrier element with an integrated probe holder and a lateral positioning system that allows displacing the electrodes parallel to the surface of the brain. By using a clamp, the carrier can be easily detached for convenient replacement of the recording electrodes during the experiment.

2.1.3. Headstage circuit board with intracellular and extracellular amplifiers and a closed-loop motor control circuit

The headstage is made of a custom flexboard (figure 2c), which includes a chip that controls the motor (NSD-2101, New Scale Technologies Inc., <http://www.newscaletech.com/>, highlighted in red), a position sensor (NSE-5310, New Scale Technologies Inc., <http://www.newscaletech.com/>, highlighted in yellow) and several operational amplifiers (AD8606, Analog Devices Inc., <http://www.analog.com>, highlighted in green) for extracellular and intracellular recordings. The printed circuit board was manufactured by Swiss PCB (<http://www.swisspcb.com>) and populated with the components by Hybrid SA (www.hybrid.ch). The exact circuit diagram is shown in Appendix C of the supplementary data. The headstage allows performing intracellular recordings using an additional intracellular amplifier (AxoClamp-2B, Axon Instruments, <http://www.moleculardevices.com>). Intracellular signals can be conditioned and tuned using blanking circuitry and capacity compensation that are integral parts of the AxoClamp system. The headstage also allows performing extracellular recordings with metal electrodes by offering a standard differential amplifier with dual output (output 1: from the reference electrode with gain 1 and output 2: amplified with gain 100 band-pass filtered (0.3-10 kHz) difference between recording and reference electrodes).

The commercial position sensor allows reading out shuttle position with a <0.5 µm resolution. The sensor itself consists uses the Hall effect to derive position information from the magnetic field generated by the

micromagnets inside the tube (see section 2.1). In brief, the sensor measures the magnetic field and transforms it to a digital position output. The sensor of size 3.98×2.57 mm in bare die form was attached to the side of the shuttle using flip chip technology.

2.1.4. The probe

The recording probe (high impedance metal electrode or glass pipette) is secured to a probe holder which can move inside a carrier. The lateral repositioning of the probe holder is realized with small rods that are fixed with Torr Seal (Varian Inc) to the carrier; the carrier itself is attached to the microdrive using a clamp operated with micro precision screws (Bergeon, <http://www.bergeon.ch>). The carriers and probes can be replaced during chronic experiments with little effort.

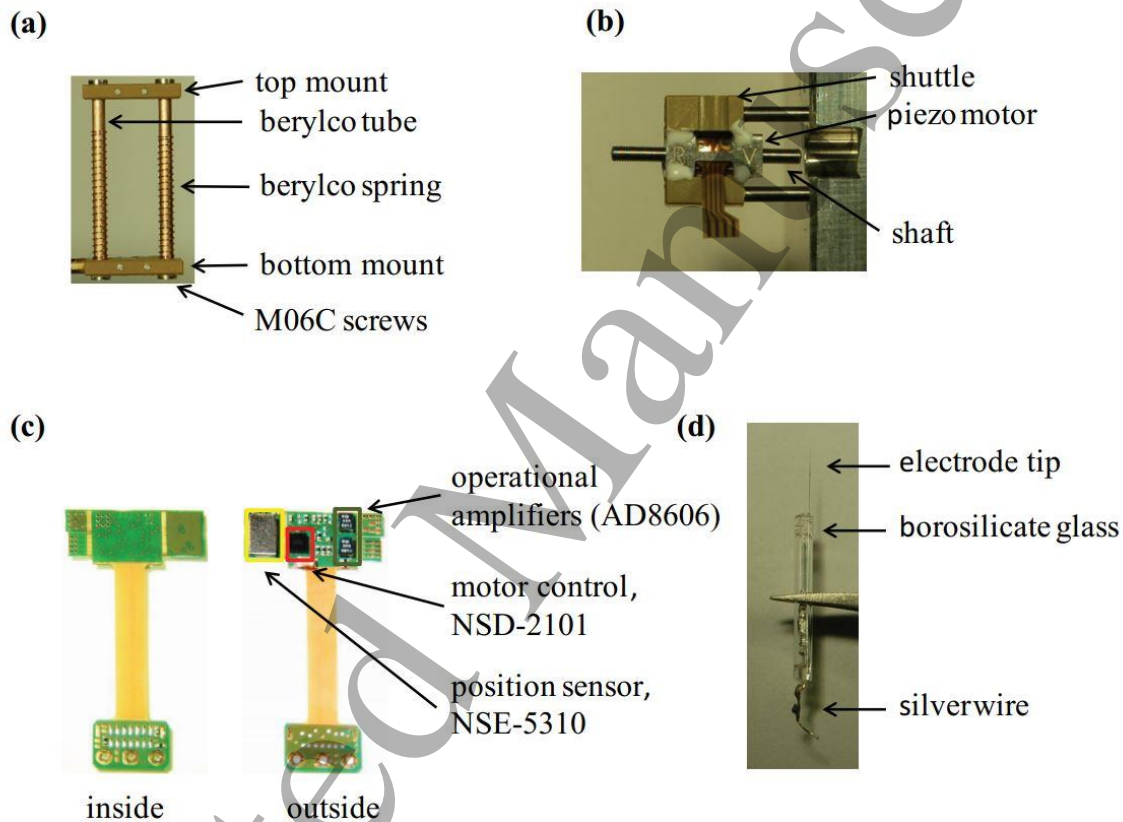


Figure 2. Microdrive components. (a) Microdrive scaffold (b) Shuttle with piezo motor (c) Circuit flexboard (d) Probe.

2.2. Software control

The control software was written in LabVIEW (National Instruments Inc.). Key features of the software are simple speed control, working range settings, and automatic target approach. The software interacts both with the Hall sensors from which the electrode position is read out and with the squiggle motor that moves the electrode in and out of the brain. The communication (I²C protocol) is supported by virtual instruments (VIs) provided by National Instruments Inc. Details are presented in Appendix D.

2.2.1. Hall sensors

From the Hall sensors (model NSE-5310, New Scale Technologies Inc.) five bytes of information are read out; these include the shuttle's position along a 2 mm long stack of magnets and a number of control parameters that allow reading out the reliability of the magnetic sensing (details in NSE-5310 datasheet). The 12 bits precision to encode a 2 mm travel range results in a position resolution of 0.5 μm .

2.2.2. Piezo motor

The piezo motor (NSD-2101, New Scale Technologies Inc.) is driven by voltage pulses. The software controller writes values in different registers of one byte each on the piezo motor driver (NSD-2101). The most commonly used parameters are the direction bit in register 2 and the 11 bits pulse count in registers 2 and 3; less often used is the pulse width in register 4 (for details see NSD-2101 datasheet).

Sending a 'move' command involves overwriting the bytes in registers 2 and 3 to define the direction of movement and the number of pulses delivered to the motor after which the motor stops (whenever the number of pulses stored in the pulse count is nonzero, the motor driver triggers a pulse and decreases the pulse count by one until the counter reaches zero and the motor becomes idle). The pulse width in register 4 (1 byte) is normally kept at its maximum value, but it can be decreased to execute very fine movements.

As a reference, a single move command set by the maximum number of pulses (2047) and maximum pulse width generates a roughly 80 μm movement within about 10-15 ms. A more practical 1 μm movement requires only about 50 pulses. In our experience, the movements generated by a fixed set of parameters are highly variable, as they depend on factors such as the nonhomogeneous physical resistance of the carrier against the guide tubes and on the direction of movement (even in repeated conditions of same direction, same starting position, and same number of pulses, two move commands may not generate the same movement – the final locations may differ by several percent, see section 3.1). The motor can at any time be instantly stopped by setting the pulse number to zero, thus resetting the motor pulse countdown.

Continuous movements are generated when the time between move commands is less than the time required to deliver all the pulses to the motor, in this case the pulse countdown never reaches zero. Because the resulting probe speed would be too high, we controlled slow movements by repeatedly sending brief pulse trains at large time intervals. For example, in a test run we moved 5 mm in about 35 seconds by sending 200 pulses once every 50 ms. Because of the large 50 ms time interval between pulse trains the pulse countdown rapidly reaches zero on each train and the motor is idle most of the time.

2.2.3. Microdrive control software and graphical user interface

We designed a microdrive control software with a graphical user interface (GUI) for convenient control of the microdrive. The GUI allows defining electrode target positions that can be precisely reached. Using the GUI, it is also possible to set the electrode range beyond which no shuttle movement is allowed. The GUI indicates the current position of the electrode, the Hall sensor's reliability, and the magnet number next to which the sensor is currently located. The microdrive control software was implemented as a LabVIEW state machine (details are presented in Appendix D).

2.3. Subjects

Three adults and one juvenile (<50 days post-hatch, dph) male zebra finches (*Taeneopygia guttata*) from our colony were used for the experiments. All the experimental procedures were approved by the

Veterinary Office of the Canton of Zurich and in accordance with the Council Directive 2010/63EU of the European Parliament on the protection of animals used for scientific purposes.

2.4. Surgery

2.4.1. Acute recordings in head-fixed animals

To test the intracellular amplifier and buzzing mechanism, intracellular recordings were performed with head-fixed anesthetized adult male zebra finches (> 90 dph). Birds were deeply anesthetized with isoflurane (1.5-3 %) and received up to four intramuscular or subcutaneous urethane injections in intervals of at least 30 minutes. Each injection consisted of 20 to 40 μ l of 20% urethane diluted in saline. We placed birds in a stereotaxic apparatus and set the head angle formed by the flat part of the skull above the beak to 65 degrees. We attached a metal plate to the skull using dental acrylic, this plate served for head fixing the bird during subsequent neural recordings. We opened a cranial window in the skull, targeting field L based on stereotaxic coordinates and by the presence of auditory responses. We inserted a silver wire into the brain in close proximity to the recording target, this wire provided the reference signal for the differential recordings. We attached the microdrive to a 55° angled micromanipulator. Using Glass pipettes filled with a 3M K-Ac solution we then performed intracellular recordings of field L responses to playback of the bird's own song. Glass pipettes were pulled with a P-97 Micropipette Puller (Sutter Instruments) and had an impedance of 110-130 M Ω . At the end of the experiments, birds were injected with an overdose of Pentobarbital and were perfused with 4% PFA.

2.4.2. Microdrive implantation surgery for chronic neural recordings in freely moving animals

Zebra finches were anaesthetized for several minutes with 1-3% Isoflurane diluted in oxygen. After achieving deep levels of anesthesia, animals were placed in a stereotactic scaffold at 65 degrees head angle and were further administrated with 1.5-3.0% isoflurane diluted in oxygen. The region of interest was identified using standard coordinates. The second bone layer above lambda was removed and lambda was used as reference point to identify the desired penetration point for recordings, around which a craniotomy was performed. After removing the bone layer (window size 0.3 x 0.3 mm), the dura was carefully removed. A recording electrode was inserted into the brain. RA neurons were identified by the presence of typical tonic firing interrupted by short bursts (Dave *et al* 1998). For adult birds we drilled several holes into the upper bone layer and delivered small amounts of very fluid dental acrylic in between the bone layers, thus providing an extremely solid base for the microdrive. In the juvenile bird, we drilled holes into the skull and inserted insect pins between the dura and the skull, these pins served as anchors for dental acrylic. We cemented the microdrive to the skull about 200 μ m above the region of interest. We inserted the reference wire for the differential recording into the brain in close proximity to the electrode. We placed the silver reference wire above the dura, covered it with paraffin wax and fixed it with dental acrylic to the skull. Thereafter, we applied paraffin wax (50% mineral oil mixed with 50% wax) to the brain surface surrounding the electrode to protect the brain surface. Additionally, we applied a layer of a silicon polymer (Kwik-Cast, World Precision Instruments, <http://www.wpiinc.com/>) to cover and seal the brain. To protect the electrode from mechanical damage, we cemented a small piece of a thin plastic transparency (0.03 g) or a bent piece of copper sheet (0.2 g) to the skull around the electrode.

2.5. Post-surgery chronic recordings

After the surgery animals were plugged to a torque-feedback commutator (Fee and Leonardo 2001). Electrodes were moved daily, starting with the first day of song recordings. Electrodes were retracted

every evening approximately 200 μm above the target area in order to avoid tissue damage. At the end of the experiments, birds were injected with an overdose of Pentobarbital and were perfused with 4% PFA.

2.6. Data acquisition

All signals were acquired using custom LabVIEW software. Neural signals from the microdrive and sound vocalizations from a microphone (Audio-technica, <http://audio-technica.com>) connected to a microphone preamplifier (Joe Meek, ThreeQ, <http://www.joemeek.com>) were band-pass filtered (300 Hz - 13 kHz) and routed to a National Instruments data acquisition card (NI PXI-6259 in PXI-1033 chassis and NI SCXI-1125 in SCXI-1000 chassis, National Instruments, <http://www.ni.com/>). Signals were digitized at 32 kHz sampling rate with 16-bits precision.

2.7. Head fixation and electrode replacement

In order to replace metal electrodes or glass pipettes, we restrained zebra finches in a foam holder and fixed their heads by clamping the two rods at the base of the microdrive to a holder (see figure 1). First, we moved the electrode out of the brain and subsequently removed the KwikCast and Paraffin to expose the brain. We carefully cleaned the craniotomy with saline. In case the dura was covered with scar tissue, we gently removed the latter. Delicate procedures were conducted with fine tools (e.g. dura tools) and observed under a stereomicroscope. In cases there was excessive dura growth, we performed additional dura treatment with 5-Fluorouracil (Sigma Aldrich, <http://www.sigmaaldrich.com>), which in monkeys was shown to reduce dural scarring (Spinks *et al* 2003). After replacing or repositioning the electrodes, we first applied Paraffin in the direct vicinity of the electrode and then KwikCast to seal the opening.

3. Results

Using a piezo motor and Hall sensor we built a lightweight microdrive that allows moving electrodes in closed loop along the dorsoventral axis. We measured the reliability and precision of motorized shuttle movements both in open loop and closed loop motor control.

3.1. Open loop shuttle movements are imprecise

We tested the reproducibility of shuttle movements in open loop control when there is no position feedback to the motor from the Hall sensor. We produced shuttle movements by a fixed number of current pulses. We found that few pulses produced very small movements. The smallest displacement achievable was less than 0.2 μm , smaller than the resolution of the sensor of 0.5 μm . To test the homogeneity of produced movements along the force of the spring and against it, we divided the total movement range into four equally sized zones. In each zone, we performed ten movement repetitions from the same starting point, five in the dorsal direction and five in the ventral direction. For each movement we triggered ten consecutive single commands of 500 pulses each, resulting in 5000 pulses per movement. After each 500-pulse command, we read out the position of the shuttle. Ideally, the shuttle displacements in all zones should be identical. However, we found substantial movement variability that was small within zones and large across zones. In the dorsal direction, the minimum distance travelled was 325 μm and the maximum distance was 389 μm . In the ventral direction, the minimum distance travelled was 82 μm and the maximum distance was 226 μm (see figure 3).

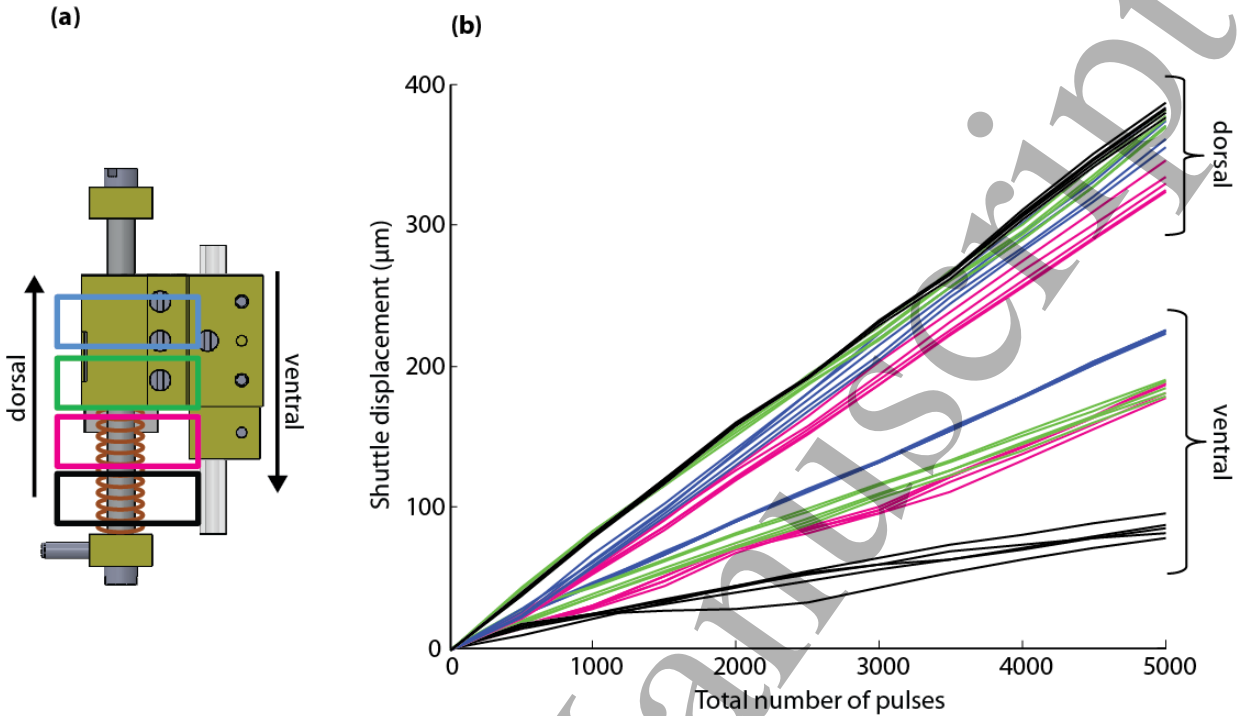


Figure 3. In open loop mode (no position feedback), the shuttle displacements produced by a fixed number of motor pulses are highly variable, illustrating the requirement for feedback control. (a) Rendered image of the microdrive. The colored squares delimit the 4 movement zones tested along the motor axis. (b) Each curve shows the shuttle displacement (μm) produced by 5000 motor pulses (one position measurement every 500 pulses). The colors indicate the zone (shown in panel a) in which the measurements were taken, five trials were performed in each zone (five curves). Measurements were taken for dorsal movements and ventral movements as shown in panel a movements against the spring (ventral) depend more strongly on the zone in which they are executed (the ratio between displacements in the black and blue zones is almost three).

In the ventral direction, the more compressed the springs were, the less distance was travelled by the shuttle. This effect was very strong, displacements were reduced by a factor of three in the bottom zone of the microdrive compared to the top zone (figure 3). Interestingly, the opposite effect was not observed in the dorsal direction, in which the spring loading did not monotonically constrain displacement magnitude. Overall, these findings reveal some surprising non-homogeneity of produced movements. The results show that displacements generated by fixed pulses are neither homogeneous nor predictable. Partly, displacements depended on the physical resistance of the shuttle against the tubes. The observed movement inconsistency calls for closed loop operation of the microdrive; it confirms our choice to control the motor using position feedback.

3.2. Shuttle movements are precise in closed loop motor control.

To test the reliability of shuttle movements in closed loop mode, we produced 200 μm target shuttle movements from three different initial positions along the motor axis. From each initial position we drove the shuttle away and back ten times and measured the endpoint offset under a stereomicroscope at 20x magnification (the focal point of the microscope objective was on the shuttle edge facing the bottom mount). We expected the shuttle to be back at the same initial position in each trial but instead we observed small offsets in endpoint positions, figure 4. From 60 offset measurements in two microdrives we found median (absolute) offsets smaller than 1 μm and a maximum offset of 4.2 μm in one microdrive and 3.6 μm in another.

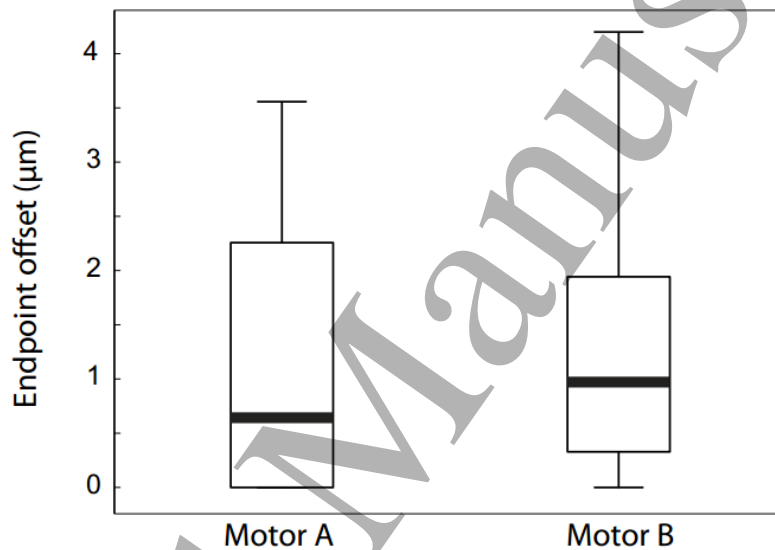


Figure 4. In closed-loop mode (with position feedback), shuttle movements are reliable. Boxplots of endpoint offsets (absolute values) resulting from 200 μm target displacements produced in four different zones (see figure 3). In both microdrives tested, the median endpoint offset (thick horizontal lines) was less than 1 μm . The boxes indicate the first and third quartiles, and the whiskers indicate the total offset range.

3.3 Electrode replacement and repositioning

All birds started to sing 1-5 days after the microdrive implantation surgery and there was no noticeable difference in song structure or singing behavior compared to before the surgery. Animals showed normal behavior and in general were not strongly influenced by the microdrive or the tether cable. We remotely controlled the electrode position in the dorso-ventral axis in freely behaving birds.

Like some older devices (Long *et al* 2010, Lee *et al* 2009, Lee *et al* 2006), our device allowed us to replace electrodes in the midst of operation. Our design also allowed repositioning of electrodes on the brain surface along both spatial dimensions. In one dimension, we used the manual screw-driven mechanism for lateral repositioning of probes within a 500 μm range. To reposition the electrode in the orthogonal dimension (with a repositioning diameter of 700 μm), we simply rotated the tube into which the electrodes were non-concentrically inserted. In combination, our design allowed us to target a wide

range of mediolateral and anteroposterior locations. We successfully replaced and repositioned both metal probes and glass pipettes.

3.4. Extracellular recordings

We recorded from single units in singing birds for up to two hours, an example extracellular signal from an HVC projection neurons recorded with a high-impedance metal electrode is shown in figure 5.

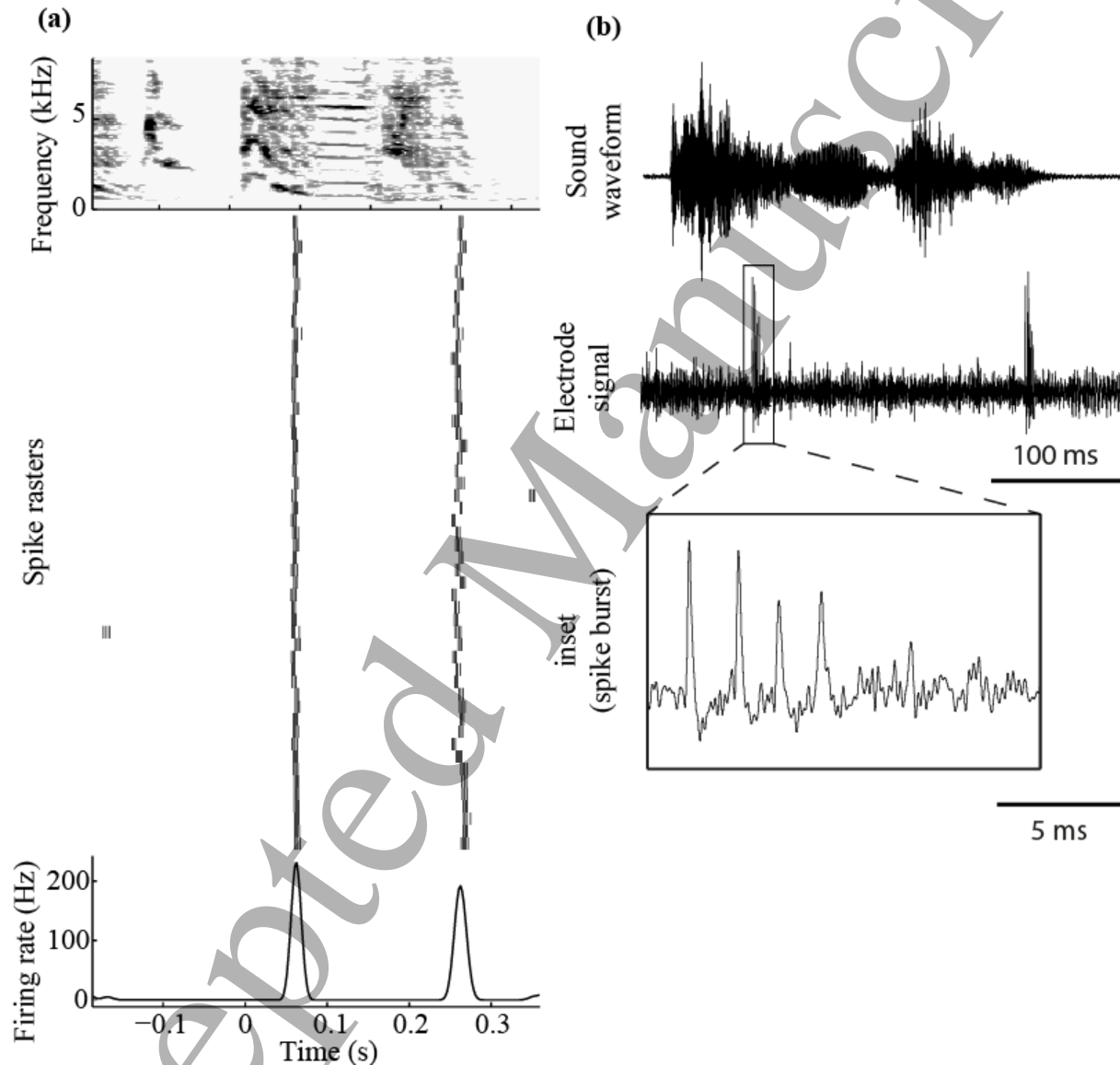


Figure 5. Song-aligned neural activity of a single HVC projection neuron. (a) Spike raster plot of a single unit firing during singing; each row depicts the action potential firing during one rendition of the stereotyped song motif in this adult bird. An example log-power sound spectrogram of the song motif is shown on top (red: high sound intensity, black: low sound intensity), the mean firing rate is depicted at the bottom. (b) Example sound amplitude (top) during song and the corresponding raw extracellular voltage trace (middle) with an inset showing the raw signal of a spike burst (bottom).

An example extracellular raw voltage trace recorded with a glass pipette is shown in figure 6.

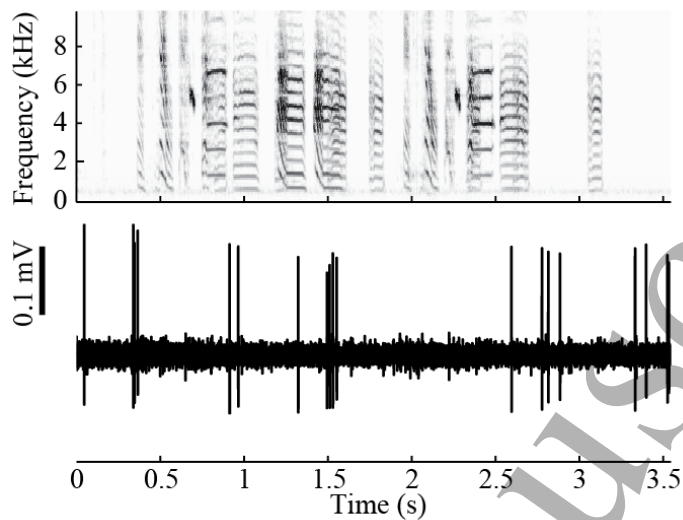


Figure 6. Log-power sound spectrogram of female-directed zebra finch song (top) and raw juxtacellular signal of a single field L neuron (bottom) recorded with a glass pipette (Borosilicate glass with filament 100-78-10; 14 M Ω filled with 3M NaCl).

3.5 Intracellular recordings

To test the intracellular amplifier we performed intracellular recordings in field L, an analogue of mammalian auditory cortex. We observed excellent signals with high signal-to-noise ratio of up to ~ 30 (figure 7) using glass pipettes filled with 3M K-Ac (Borosilicate glass with filament 100-50-10; 110-140 M Ω). To penetrate a cell, we advanced the pipette until we observed a small deflection in the electrode potential, indicating that the pipette tip was pressing against a cell membrane. At this point the "buzzing" function was used to penetrate the cell. The "buzzing" function drives a brief and large current oscillation through the micropipette by temporarily increasing the capacitance neutralization beyond its stable range (see figure 8). The duration of this oscillation can be remotely set by the user to discrete values between 100 μ s and 500 ms. This method can also help to clear blocked pipette tips. The buzzing mechanism may involve attraction between charges at the tip of the electrode and bound charges on the inside of the membrane.

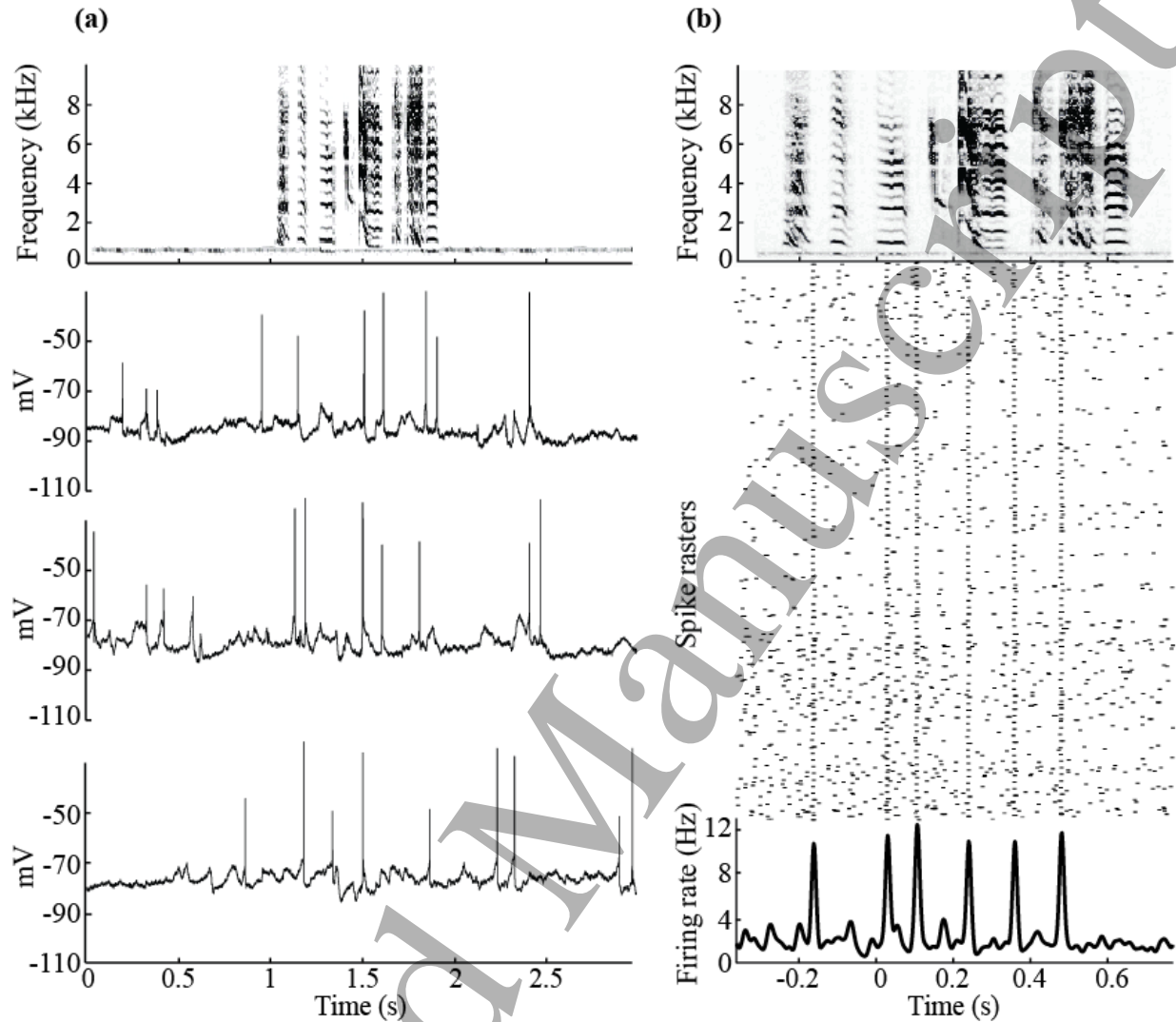
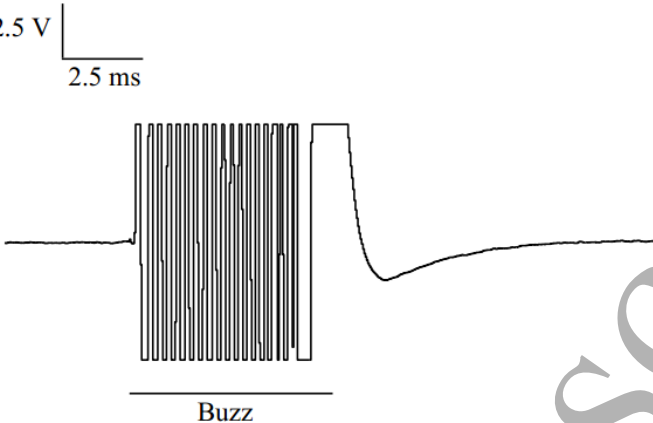


Figure 7. Song playback-aligned intracellular activity (a) Examples of three raw intracellular voltage traces of a field L neuron responding to playback of the bird's own song (spectrogram shown on top). (b) Aligned spike-raster plot for the same neuron, each row depicts the action potential firing during one rendition of the song motif (spectrogram shown on top). The mean firing rate is depicted at the bottom.

1
2
3
4
5
6
7
8
9
10
11
12
13
14
15
16
17
18
19
20
21
22
23
24
25
26
27
28
29
30
31
32
33
34
35
36
37
38
39
40
41
42
43
44
45
46
47
48
49
50
51
52
53
54
55
56
57
58
59
60



2.5 V
2.5 ms

Buzz

Figure 8. The buzzing function to clean clogged pipettes. Examples raw voltage trace recorded from an anesthetized animal with a glass pipette (125 M Ω). The peak-to-peak voltage amplitude is 10 V (is clipped at ± 5 V ADC rails). The current oscillation through the micropipette is clearly visible; the manually set duration of the buzz is indicated at the bottom.

3.6 Other applications

The versatile design of the microdrive allowed for some applications other than neural recordings in freely moving animals. For example, we have used a modified version of the microdrive (with a modified scaffold, see Appendix C of the supplementary information) as a one-axis motorized micromanipulator that is convenient in applications where there are tight space requirements. Furthermore, we tested the seven unit-gain followers on the microdrive board. These followers could be used to record diverse physiological signals. For example, they could be connected to diverse sensors such as thermistors for measuring brain temperature, pressure sensors for measuring respiration, etc.

4. Discussion

We designed a microdrive for chronic neural recordings that combines several key advantages of earlier designs (Fee & Leonardo 2001; Battaglia et al. 2009; Long et al. 2010; Lee et al. 2006; Lee et al. 2009). Using a single device, we have performed successful recordings using both metal electrodes and glass pipettes. While our drive is arguably one of the most versatile lightweight drives documented in the literature, there are several desirable features for future development. A simple candidate feature could be the active holding of the electrode in a given position. We have observed that overnight, and with vibrations generated by a bird's movement, the electrode gradually moved away from the position where it had been left, in the direction in which the springs are pushing (dorsal). It may be desirable, for example overnight, to compensate for possible electrode drift caused by repeated head movements. The reasons for not implementing this feature currently are related to safety considerations (not operating the microdrive in the user's absence).

A more extensive implementation of automatic control could be useful during neural recordings, for example, to hold a single cell over a long period of time. This feature would require frequent readings of the position sensor and occasional motor adjustments, both of which would generate noise on the electrode signal that might impair the neural recordings. Therefore, such a feature would ideally have to be implemented in a closed loop with behavioral readouts, for example, to suppress electrode repositioning during singing or other behaviors of interest.

1
2
3 On the hardware side, it would be desirable to allow recordings from more than a single electrode. For
4 example, it should be possible to revise the design to provide room for headstage electronics such as the
5 RHA2116 (Intan Technologies, Los Angeles, USA), which would provide up to 16 independent recording
6 channels. In this case, closed-loop repositioning could be implemented via feedback from the electrodes.
7 For example, it would be convenient to let the system perform dorsal penetrations in small increments
8 whenever none of the electrodes or tetrodes contains satisfactory signals. Possibly, such an automated
9 solution might allow electrophysiologists to overcome brain-access bottlenecks which currently limit the
10 number of neurons recorded in freely behaving animals.
11
12
13

14 **Acknowledgements**

15 We thank Irina Panova for the help with the microdrive PCB design. This work was funded by the Swiss
16 National Science Foundation (grant 31003A_127024) and by the European Research Council under the
17 European Community's Seventh Framework Programme (ERC Grant AdG 268911 FP7/2007-2013).
18
19
20
21
22
23
24
25
26
27
28
29
30
31
32
33
34
35
36
37
38
39
40
41
42
43
44
45
46
47
48
49
50
51
52
53
54
55
56
57
58
59
60

References

- Ainsworth A & O'Keefe J, 1977 A lightweight microdrive for the simultaneous recording of several units in the awake, freely moving rat. *J Physiol* **269** 8–10.
- Battaglia FP, Kalenscher T, Cabral H, Winkel J, Bos J, Manuputy R, van Lieshout T, Pinkse F, Beukers H & Pennartz C, 2009 The Lantern: An ultra-light micro-drive for multi-tetrode recordings in mice and other small animals *Journal of Neuroscience Methods* **178** 291–300.
- Brecht M, Schneider M, Sakmann B & Margrie TW, 2004 Whisker movements evoked by stimulation of single pyramidal cells in rat motor cortex. *Nature* **427** 704–710.
- Dave AS, Yu AC & Margoliash D, 1998 Behavioral state modulation of auditory activity in a vocal motor system. *Science (New York, N.Y.)* **282** 2250–4. Available at: <http://www.ncbi.nlm.nih.gov/pubmed/9856946>.
- Deadwyler S, Biela J, Rose G, West M & Lynch G, 1979 q 752–754.
- Fee MS & Leonardo A, 2001 Miniature motorized microdrive and commutator system for chronic neural recording in small animals. *Journal of neuroscience methods* **112** 83–94.
- Foster JD, Nuyujukian P, Freifeld O, Gao H, Walker R, Ryu S, Meng T, Murmann B, Black M & Shenoy K V, 2014 A freely-moving monkey treadmill model. *Journal of neural engineering* **11** 46020. Available at: <http://www.ncbi.nlm.nih.gov/pubmed/24995476> [Accessed June 21, 2016].
- Hafting T, Fyhn M, Molden S, Moser M-B & Moser EI, 2005 Microstructure of a spatial map in the entorhinal cortex. *Nature* **436** 801–6.
- Hahnloser RHR, Kozhevnikov A & Fee MS, 2002 An ultra-sparse code underlies the generation of neural sequences in a songbird. *Nature* **419** 65–70. Available at: <http://www.ncbi.nlm.nih.gov/pubmed/12214232>.
- Kozhevnikov A & Fee MS, 2007 Singing-Related Activity of Identified HVC Neurons in the Zebra Finch *Journal of Neurophysiology* **97** 4271–4283.
- Lee AK, Epsztein J & Brecht M, 2009 Head-anchored whole-cell recordings in freely moving rats. *Nat. Protoc.* **4** 385–392.
- Lee AK, Manns ID, Sakmann B & Brecht M, 2006 Whole-Cell Recordings in Freely Moving Rats *Neuron* **51** 399–407.
- Lever C, Wills T, Cacucci F, Burgess N & O'Keefe J, 2002 Long-term plasticity in hippocampal place-cell representation of environmental geometry. *Nature* **416** 90–94.
- Long MA, Jin DZ & Fee MS, 2010 Support for a synaptic chain model of neuronal sequence generation. *Nature* **468** 394–399. Available at: <http://www.ncbi.nlm.nih.gov/pubmed/20972420> [Accessed October 26, 2010].
- Márton G, Baracska P, Cseri B, Plósz B, Juhász G, Fekete Z & Pongrácz A, 2016 A silicon-based microelectrode array with a microdrive for monitoring brainstem regions of freely moving rats *Journal of Neural Engineering* **13** 26025. Available at: <http://stacks.iop.org/1741-2552/13/i=2/a=026025?key=crossref.096c02d2c31fead9c9e91457a094580b>.
- McCasland JS, 1987 Neuronal control of bird song production. *The Journal of Neuroscience* **7** 23–39. Available at: <http://www.ncbi.nlm.nih.gov/pubmed/3806194>.

- 1
2
3
4
5
6
7
8
9
10
11
12
13
14
15
16
17
18
19
20
21
22
23
24
25
26
27
28
29
30
31
32
33
34
35
36
37
38
39
40
41
42
43
44
45
46
47
48
49
50
51
52
53
54
55
56
57
58
59
60
- McCasland JS & Konishi M, 1981 Interaction between Auditory and Motor Activities in an Avian Song Control Nucleus *Proceedings of the National Academy of Sciences* **78** 7815–7819. Available at: <http://www.pnas.org/cgi/content/abstract/78/12/7815> [Accessed August 20, 2011].
- O’Keefe J & Dostrovsky J, 1971 The hippocampus as a spatial map . Preliminary evidence from unit activity in the freely-moving rat **34** 171–175.
- Prather JF, Peters S, Nowicki S & Mooney R, 2008 Precise auditory-vocal mirroring in neurons for learned vocal communication. *Nature* **451** 305–10. Available at: <http://www.ncbi.nlm.nih.gov/pubmed/18202651>.
- Schneider DM, Nelson A & Mooney R, 2014 A synaptic and circuit basis for corollary discharge in the auditory cortex *Nature* **513** 189–194.
- Spinks RL, Baker SN, Jackson A, Khaw PT & Lemon RN, 2003 Problem of dural scarring in recording from awake, behaving monkeys: a solution using 5-fluorouracil. *Journal of neurophysiology* **90** 1324–1332.
- Tolias AS, Ecker AS, Siapas AG, Hoenselaar A, Keliris GA & Logothetis NK, 2007 Recording chronically from the same neurons in awake, behaving primates. *Journal of neurophysiology* **98** 3780–90.
- Venkatachalam S, Fee MS & Kleinfeld D, 1999 Ultra-miniature headstage with 6-channel drive and vacuum-assisted micro-wire implantation for chronic recording from the neocortex. *Journal of neuroscience methods* **90** 37–46.
- Yamamoto J & Wilson MA, 2008 Large-scale chronically implantable precision motorized microdrive array for freely behaving animals. *Journal of neurophysiology* **100** 2430–40.
- Yang S, Cho J, Lee S, Park K, Kim J, Huh Y, Yoon ES & Shin HS, 2011 Feedback controlled piezo-motor microdrive for accurate electrode positioning in chronic single unit recording in behaving mice *Journal of Neuroscience Methods* **195** 117–127.
- Yin M, Borton DA, Komar J, Agha N, Lu Y, Li H, Laurens J, Lang Y, Li Q, Bull C, Larson L, Rosler D, Bezard E, Courtine G & Nurmikko A V, 2014 Wireless neurosensor for full-spectrum electrophysiology recordings during free behavior. *Neuron* **84** 1170–82. Available at: <http://www.ncbi.nlm.nih.gov/pubmed/25482026> [Accessed June 21, 2016].